



# In Vitro Antioxidant, Antipathogenicity and Cytotoxicity Effect of Silver Nanoparticles Fabricated by Onion (*Allium cepa* L.) Peel Extract

Rajkumar Krishnasamy Sekar<sup>1</sup> · Arun Sridhar<sup>1</sup> · Balaji Perumalsamy<sup>2</sup> · Dinesh Babu Manikandan<sup>1</sup> · Thirumurugan Ramasamy<sup>1,2</sup>

Published online: 22 November 2019

© Springer Science+Business Media, LLC, part of Springer Nature 2019

## Abstract

In this study, we emphasize a rapid and cost-effective biogenic approach for the synthesis of silver nanoparticles (AgNPs) using an aqueous extract of onion (*Allium cepa* L.) peel (brown skin) acting as a reducing and capping agent. The synthesized AgNPs were characterized by UV-visible spectroscopy, X-ray diffraction (XRD), Fourier transform infrared spectroscopy (FT-IR), transmission electron microscopy (TEM), and energy-dispersive X-ray spectroscopy (EDS) analysis. The morphology of synthesized AgNPs was a spherical shape, cubic structure with an average particle size range of 33–50 nm. The AgNPs have higher antioxidant activities (2,2-diphenyl-1-picrylhydrazyl (DPPH) and 2,2'-azino-bis(3-ethylbenzothiazoline-6-sulphonic acid) (ABTs) when compared with ascorbic acid (vitamin C). The synthesized AgNPs have strong antipathogenic activity towards foodborne illness-causing bacterial pathogens of Gram-positive (*Bacillus* sp., *Staphylococcus aureus*, and *Corynebacterium* sp.) and Gram-negative (*Escherichia coli*, *Salmonella* sp., and *Vibrio cholerae*) organisms. Furthermore, the AgNPs have the potential anti-proliferative action on A549 lung cancer cell lines, suggesting a novel chemotherapeutic agent against human lung cancer.

**Keywords** Quercetin · A549 cancer cell line · Mitochondrial swelling · ROS generation · Nuclear fragmentation

## 1 Introduction

In recent years, nanoparticles (NPs) have been in high demand due to their superior properties and various fields of applications in biomedical, catalytic, energy and materials, antimicrobial, and plant growth metabolism [1, 2]. Nanoparticles have tremendous scientific attention, and they fill the gap between micro materials and atomic or molecular structures [3]. The aqueous (SiO<sub>2</sub>), hybrid (titanium alloy and ferromagnetic), and column-shaped (CuO) NPs effectively play a role in the heat transportation process [4–6]. The development of metallic NPs leads to new, improved properties like size, morphology, and distribution [7]. In earlier times, numerous methods

were developed to produce nano-based materials physically, chemically, and biologically [8]. The physical method of synthesizing NPs requires high temperature and pressure [9] and also releases a lot of thermal energy during the synthesis process [10]. The chemical method may lead toxicity to the environment, especially for the aquatic eco-system, when it reaches higher concentrations [11]. Certain limitations were faced while pre-synthesization and post-synthesization of NPs by physical and chemical methods can be reduced by biological approach.

Nowadays, biological syntheses of metal oxide NPs are growing in attention to the field of bionanoscience. It emphasizes the use of natural organisms: which not only offer a reliable, simple, and low production cost but are eco-friendly as well. Several researchers have reported the synthesis of biogenic NPs by various plant extracts, which have phytochemical constituents used as reducing and capping agents with medicinal properties. The biogenic NPs have a wide spectrum of applications, including biosensors, antimicrobial agents, drug delivery, gene therapy, and cancer treatment [12]. The synthesis mechanism of biogenic NPs mainly depends on the phytochemical compounds, phenols, flavonoids, alkaloids, terpenoids, tannins, carbohydrates, and saponins [13].

✉ Thirumurugan Ramasamy  
ramthiru72@bdu.ac.in

<sup>1</sup> Laboratory of Aquabiotics/Nanoscience, Department of Animal Science, School of Life Sciences, Bharathidasan University, Tiruchirappalli, Tamil Nadu 620 024, India

<sup>2</sup> UGC-National Centre for Alternatives to Animal Experiments (NCAAE), Bharathidasan University, Tiruchirappalli, Tamil Nadu 620 024, India

Silver nanoparticles (AgNPs) can diffract and absorb the light as well as exhibit color, depending on the morphology, size, and shape. AgNPs are gaining a lot of attention due to its unique properties like catalytic, optical, and antimicrobial properties [14]. Presently, AgNPs were synthesized by using different biological methods, *Paederia foetida* L. leaf extract [15], *Ribes nigrum* fruit extract [16], *Trigonella foenum-graecum* leaf extract [17], *Tribulus terrestris* L. extract [18], *Datura innoxia* flower extract [19], and *Diospyros montana* leaf extract [20]. Usually, biogenic-synthesized AgNPs have anti-proliferative activity against cancer cell lines in a dose-dependent manner. It associates strongly with an increased level of reactive oxygen species (ROS), which leads to loss of mitochondrial membrane integrity.

Antioxidant enzymes play an essential role in protecting the body from adverse effects generated by free radicals during normal metabolism [21]. The research shows that the plant sources possess higher antioxidants, which neutralize the free radicals and decompose the peroxides [22]. Therefore, the biogenic nanoparticles have antioxidant activities due to superior adsorption of the antioxidant material derived from the extract on the surface of the NPs [23]. A small quantity of silver is safe for human cells, but it is toxic to the bacteria and fungi [24]. In spite of the antibacterial activities of AgNPs that have been proven, the actual mechanism is not yet clear. NPs may inactivate the microbes by inhibiting their enzymes, proteins, or DNA [25]. Cancer is one of the most common causes of death worldwide from the beginning of the twenty-first century. Therefore, we need to develop less toxic, inexpensive, and more effective therapeutic agents to treat cancer.

Onion (*Allium cepa* L.) is the second most important horticultural crop and consumed throughout the world. Several studies suggested that they have biomedical applications due to their higher content of organosulfur compounds [26–30]. The brown skin (dry outer layer) of an onion has functional ingredients rich in dietary fiber, phenolics, and flavonoids with antioxidant activity and high concentration of quercetin and calcium [31]. Prakash et al. [32] reported that the dry outer layer showed higher free radical scavenging and antioxidant activity than the other layers of an onion. The outer skin of an onion exhibited more active antioxidant properties than garlic [33].

Many reports have summarized the synthesis of silver nanoparticles from the onion as a source of the reducing agent [34, 35]. The synthesized AgNPs have antioxidant activities and control cardiac arrhythmic, tumor inhibition, antidiabetes, and antibacterial [32, 33, 36]. In consideration of the above reports, no attempt was made to formulate the AgNPs by onion peel (brown skin). But herein, we described the synthesis of AgNPs using onion peel extract as a reducing and capping agent. Due to the above said reasons, the present study has designed to use onion peel extract for the synthesis of

AgNPs from silver nitrates and test its antioxidant, anticancer (lung cell line), and antibacterial activity foodborne illness-causing bacteria such as *Bacillus* sp., *Staphylococcus aureus*, *Corynebacterium* sp., *Escherichia coli*, *Salmonella* sp., and *Vibrio cholerae* were evaluated.

## 2 Materials and Methods

### 2.1 Collection and Preparation of Peel Extract

The fresh onion (*Allium cepa* L.) peels were collected from the local market of Tiruchirappalli, Tamil Nadu, India. Peels were cleaned with double distilled water and shadow dried. Five grams of onion peels were transferred to a 250-mL Erlenmeyer flask, and 100 mL double distilled water was added and boiled at 60 °C for 20 min to get the aqueous extract. Then, the extract was filtered by using Whatman no.1 filter paper, and refrigerated at 4 °C for further use.

### 2.2 Synthesis of Silver Nanoparticles

An aqueous solution (0.001 M) of AgNO<sub>3</sub> was prepared using 100 mL double distilled water. Ten milliliters of onion peel extract was added to the solution of AgNO<sub>3</sub> by dropwise while stirring magnetically at 300 rpm until the solution becomes dark brownish color. The color change indicates the formation of colloidal AgNPs, and it was analyzed by UV-visible spectroscopy. The obtained colloidal AgNPs were centrifuged at 6000 rpm for 20 min. The centrifuged pellets were washed several times with double distilled water to the removal of excess, unconverted silver ion residues and other unwanted materials. Finally, the pellets were air-dried and collected in powder form for characterization.

### 2.3 Characterization of Synthesized Nanoparticles

#### 2.3.1 UV-Vis Spectra Analysis

The formation and stability of synthesized AgNPs were analyzed in Synergy HT Multimode Reader (BioTek, Winooski, VT, USA), with the absorption range of 300–700 nm wavelength. The absorption spectrum of the reaction solution was recorded at different time intervals.

#### 2.3.2 X-Ray Diffraction Analysis

The crystalline metallic pattern of AgNPs powder was carried through an X-ray diffractometer (PANalytical X'Pert Pro Powder X'Celerator Diffractometer, Netherlands) and operated with a voltage of 40 kV and current of 40 mA with Cu K<sub>α</sub> radiation (1.5406 Å). The scanning was done in the range of 10–80°.

### 2.3.3 FT-IR Spectrum Analysis

The functional groups of biogenic AgNPs were recorded using FT-IR spectrophotometer Perkin Elmer Spectrum Version 10.03.09 with the KBr pellet method. The spectrum wavenumber frequency ranges from 4000 to 500  $\text{cm}^{-1}$ . Measurements were recorded in transmittance (% T) mode.

### 2.3.4 TEM with EDS Analysis

Transmission electron microscopy (TEM) was applied for the morphological analysis of biogenic-synthesized AgNPs. The required volume of the sample was prepared and dispersed on carbon-coated copper grids and allowed to dry at room temperature. The TEM images and measurements were analyzed on FEI-TECNAI G2 F20, which was operated at 200 kV. At the same time, the energy dispersive spectrum (EDS) was also recorded.

## 2.4 In Vitro Antioxidant Assay

### 2.4.1 Assay of 2,2-Diphenyl-1-Picrylhydrazyl

The radical scavenging activity of AgNPs against 2,2-diphenyl-1-picrylhydrazyl (DPPH) was determined by a modified method of Brand-Williams et al. [37]. In brief, different concentrations (20, 40, 60, 80, and 100  $\mu\text{g/mL}$ ) of an aqueous solution of AgNPs were prepared in 96-well plates with ascorbic acid as standard. One millimolar of freshly prepared methanolic extract of the DPPH solution was added to each well. The mixture solution was incubated at room temperature for 30 min in dark condition. Change of color from violet to yellow was observed. Synergy HT Multimode reader was used to measure the absorbance of the mixture at 517 nm. Then, the scavenging ability was calculated by the following equation.

$$\% \text{ Scavenging} = \frac{A_c - A_s}{A_c} \times 100$$

where  $A_c$  is the absorbance of the methanolic DPPH and  $A_s$  is the absorbance of test samples.

### 2.4.2 Assay of 2,2'-Azinobis-(3-Ethylbenzothiazoline-6-Sulfonic Acid)

2,2'-Azinobis-(3-ethylbenzothiazoline-6-sulfonic acid) (ABTS) assay was performed according to the method of Roberta et al. [38] with slight modifications. The ABTS radical cation was prepared by dissolving 7 mM of ABTS and 2.45 mM potassium persulfate and allow the mixture to stand in the dark at room temperature for 12–16 h to produce ABTS radical (ABTS $\bullet$ +). This solution was diluted with ethanol to an absorbance of 0.700 ( $\pm 0.05$ ) at 734 nm. After the

measurement, different concentrations (20, 40, 60, 80, and 100  $\mu\text{g/mL}$ ) of an aqueous solution of AgNPs were prepared with ascorbic acid as standard and 100  $\mu\text{L}$  of ABTS solution was added to the respective wells. The absorbance was taken for 6 min with an interval of 1 min. Then, the antioxidant activity of the sample was calculated by the following equation.

$$\% \text{ Scavenging} = \frac{A_c - A_s}{A_c} \times 100$$

where  $A_c$  is the absorbance of the ABTS $\bullet$ + and  $A_s$  is the absorbance of test samples.

## 2.5 Determination of Antipathogenic Activity

The antipathogenic activity of biogenic AgNPs was determined through the agar well diffusion method. Twelve hours of clinical isolates, Gram-positive (*Bacillus* sp., *S. aureus*, and *Corynebacterium* sp.) and Gram-negative (*E. coli*, *Salmonella* sp., and *V. cholerae*) organisms were swabbed over the freshly prepared nutrient agar plates. Then, wells (6 mm) were made and different concentrations of AgNPs (25, 50, 75, and 100  $\mu\text{g/mL}$ ) and a positive control (streptomycin (1 mg/ml)) were added to respective wells. After overnight incubation 37  $^{\circ}\text{C}$ , the zone of inhibition was determined by measuring the diameter (mm) of the clear zone around the well, and the mean values were recorded. The activity was performed in triplicates.

## 2.6 Cell Culture

A human lung cancer A549 cell line was obtained from the National Centre for Cell Science (NCCS), Pune, India. The cells were cultured in Dulbecco's Modified Eagle Medium (DMEM), high glucose (Sigma-Aldrich, USA) medium supplemented with 10% FBS (fetal bovine serum) (Gibco), and 1% antibiotics (penicillin-streptomycin, Gibco), in a humidified atmosphere of 5%  $\text{CO}_2$  at 37  $^{\circ}\text{C}$  in  $\text{CO}_2$  incubator (Thermo Scientific, USA).

## 2.7 In Vitro Cytotoxicity Assay (MTT Assay)

The cytotoxicity of synthesized AgNPs on A549 cells was determined by MTT assay [39]. A549 cells were plated in 100  $\mu\text{L}$  of a respective medium at a density of  $5 \times 10^3$  cells/well in 96 flat bottomed well plates. After 24-h incubation, AgNPs were added in concentrations ranging from 0 to 200  $\mu\text{g/mL}$  to study the cytotoxic effect. The media was replaced after 24-h incubation with 20  $\mu\text{L}$  of MTT (5 mg/mL in PBS) and incubated for 4 h. Then, the solution was discarded, and the purple MTT-formazan was dissolved in 100  $\mu\text{L}$  of DMSO. Optical density of MTT-formazan was measured at a wavelength of 550 nm with a reference wavelength of

690 nm using Synergy HT Multimode Reader. The experiment was performed in triplicates. The percentage of inhibition was calculated by the following formula:

$$\% \text{ inhibition} = \frac{\text{mean OD of control (Untreated cells)} - \text{mean OD of treated cells}}{\text{mean OD of control (Untreated cells)}} \times 100$$

## 2.8 Dual AO/EB Staining

Apoptotic morphology was investigated through the AO/EB dual staining method as described by Spector et al. [40] with some modifications. Cells (A549) were plated at a density of  $5 \times 10^5$  cells/well in 96-well plates, and cells allowed to adhere for 24 h at 37 °C. Then, the cells were treated with the IC<sub>50</sub> concentration of AgNPs for 24 h. After the end of the treatment, cells were washed with PBS and exposed to 25 μL of AO/EB solution on a microscopic slide and viewed under a fluorescent microscope (Carl Zeiss, Axioscope2plus).

## 2.9 Hoechst 33258 Staining

Cell pathology was detected by staining the nuclear chromatin of trypsinized A549 cells [41]. A549 cells of  $5 \times 10^5$  cells/mL were seeded in a 6-well plate and treated with 24 h of IC<sub>50</sub> concentrations of AgNPs. After incubation, the control and AgNPs-treated cells were harvested and stained with Hoechst 33258 stain (1 mg/mL) at 37 °C. After 10 min of incubation, a drop of cell suspension was placed on a glass slide and covered by a coverslip. Approximately 300 cells were observed in the fluorescent microscope (Carl Zeiss, Axioscope2plus) with excitation and emission wavelength of 350 and 460 nm respectively.

## 2.10 Mitochondrial Membrane Potential (MMP)

The mitochondrial depolarization pattern of the A549 cells was analyzed by Rhodamine 123 staining [42] in the populations of apoptotic cells. The 24-h IC<sub>50</sub> concentration of AgNPs-treated A549 cancer cell lines ( $5 \times 10^5$  cells/mL) was mixed with 25 μL of Rhodamine 123 solution (1 mg/mL), and a drop of the mixture solution was placed on a microscope slide. The mitochondrial membrane disruption of the cells was observed under a fluorescent microscope (Carl Zeiss, Axioscope2plus) fitted with a UV filter of 377–355 nm.

## 2.11 Statistical Analysis

All the experimental data were expressed as the mean ± standard deviation. Statistical significance ( $P < 0.05$ ) between samples was determined by one-way analysis of variance (ANOVA) using SPSS 16.0 software (SPSS, Chicago, IL, USA).

## 3 Results and Discussion

### 3.1 UV-Vis Spectroscopy Analysis

The optical properties of AgNPs were studied by using UV-vis spectroscopy (Fig. 1). The synthesis reaction was monitored 0 to 30 min, and the color change occurred by the presence of pigments and secondary metabolites in the onion peel extract. In this case, the reduction of silver ions into AgNPs occurs rapidly. More than 70% reduction of Ag<sup>+</sup> ions was completed within 30 min after the addition of the onion peel extract to the AgNO<sub>3</sub> solution. Earlier reports showed the synthesis of

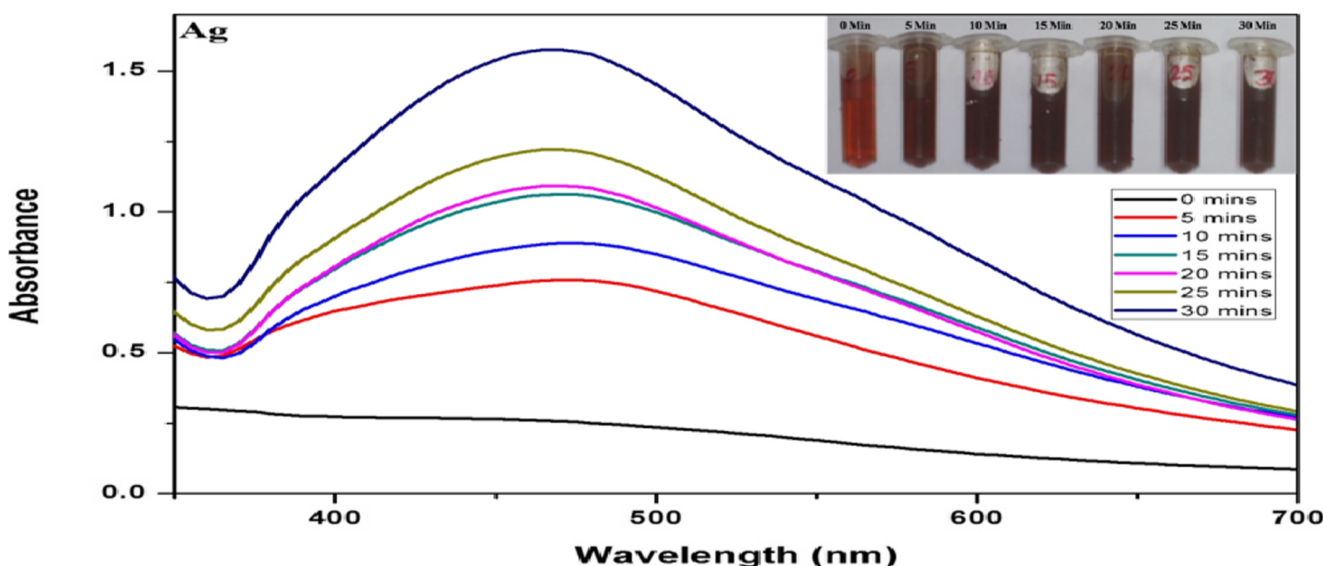


Fig. 1 UV-vis absorption spectra of AgNPs and inset photograph represented the different reaction time



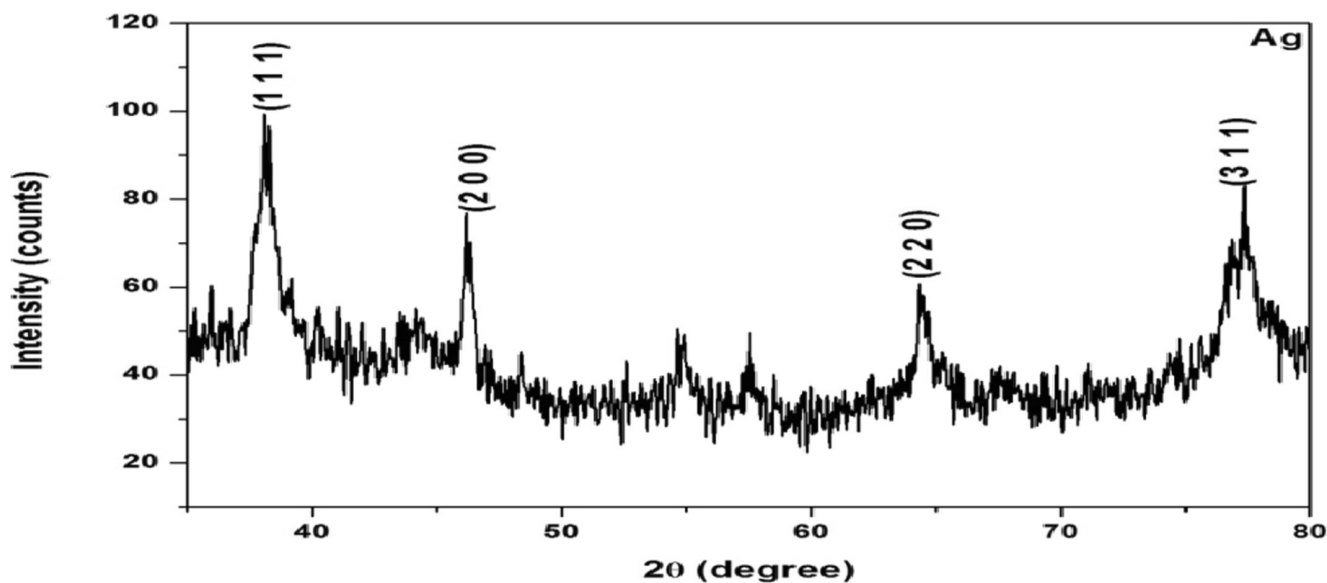


Fig. 2 XRD pattern of green synthesized silver nanoparticles

AgNPs using biological sources as the reducing agent, the time required for complete reduction of the  $\text{Ag}^+$  ions between 24 to 120 h [43–46]. The formation of AgNPs may be due to the phenolics, flavonoids, quercetin aglycone, and calcium in the peel of an onion. It has been reported that the onion wastes (*Allium cepa* L.) contain dietary fiber and bioactive compounds [31]. AgNPs exhibit dark brownish color arising due to the excitation of surface plasmon resonance (SPR) in the visible region ranging from 350 to 700 nm. The results were in agreement with *Dimocarpus longan* Lour. peel extract-synthesized AgNPs [47]. The wavelength region has a typical SPR absorption band of synthesized AgNPs at a wavelength of maxima ( $\lambda$  max) at around 466 nm (Fig. 1). The previous

study of biosynthesized AgNPs showed surface plasmon resonance at around 460 nm [48].

### 3.2 X-Ray Diffraction Measurement

The AgNPs X-ray diffraction (XRD) pattern was indexed completely with the results supporting that the prepared material exhibited a face-centered cubic (fcc) structure of silver (JCPDS card no. 03-0921) with a bio-organic phase (Fig. 2). The Ag XRD pattern revealed (1 1 1), (2 0 0), (2 2 0), and (3 1 1) planes were located at the  $2\theta$  at 38.07°, 46.18°, 64.32°, and 77.35°, respectively, and confirmed the fcc structure of AgNPs, which might have resulted from the bioactive

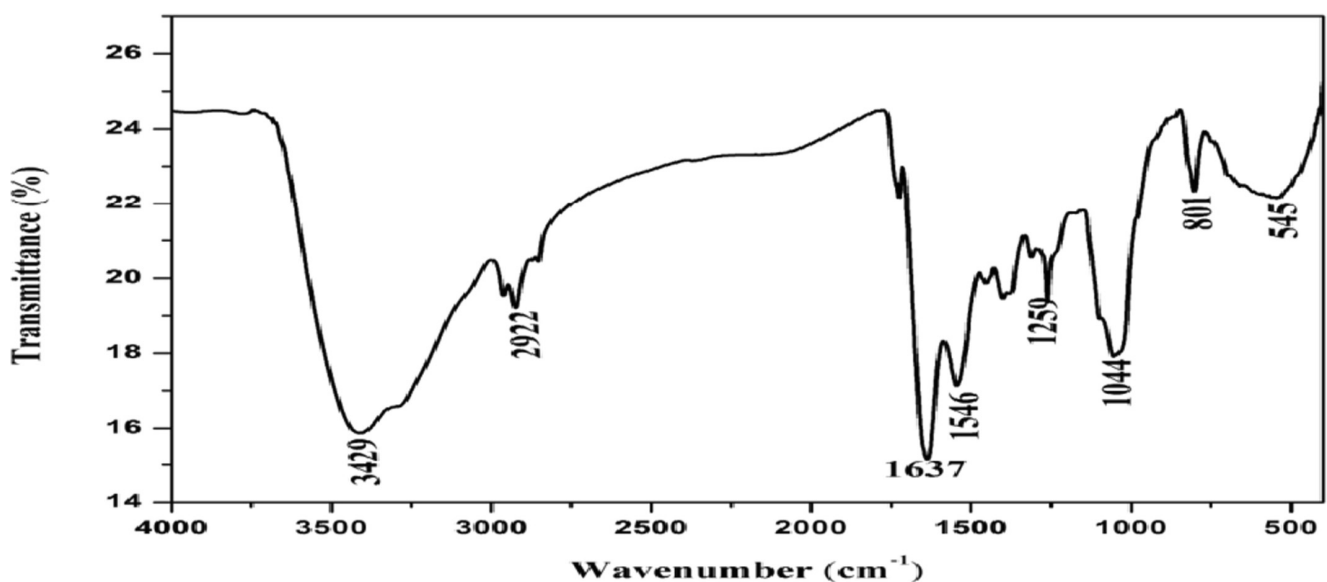


Fig. 3 FT-IR spectrum of synthesized AgNPs by aqueous onion peel extract

compounds in the onion peel extract. Additional diffraction peaks corresponding to biological matters were detected; this was normal in the biological method. This statement was agreed for *Ganoderma neo-japonicum* Imazeki and *Gossypium hirsutum* extract-based syntheses AgNPs [49, 50]. Similar results were also observed in different plant extract-synthesized AgNPs [51, 52]. The average particle size of AgNPs calculated by the Scherrer equation, i.e.,

$$D = K\lambda / \beta \cos\theta$$

In the above equation,  $D$  is particle size,  $\lambda$  is X-ray wavelength (0.15426 nm),  $\beta$  is FWHM, and  $\theta$  is Bragg's angle. In

the present study, the XRD pattern of AgNPs showed that the average particle size is 33 nm. In comparison with the previous report [50], the AgNPs were slightly smaller, with an XRD modal diameter of 12 nm.

### 3.3 Fourier Transform Infrared Spectroscopy Analysis

The Fourier transform infrared spectroscopy (FT-IR) spectrum of AgNPs was showed in Fig. 3. The brown skin of an onion peel extract contains different phytochemical constituents such as dietary fiber, phenolics, and flavonoids [31]. This phytochemical plays an important role in the formation and stabilization of AgNPs. Two distinctive peaks at 3429 and

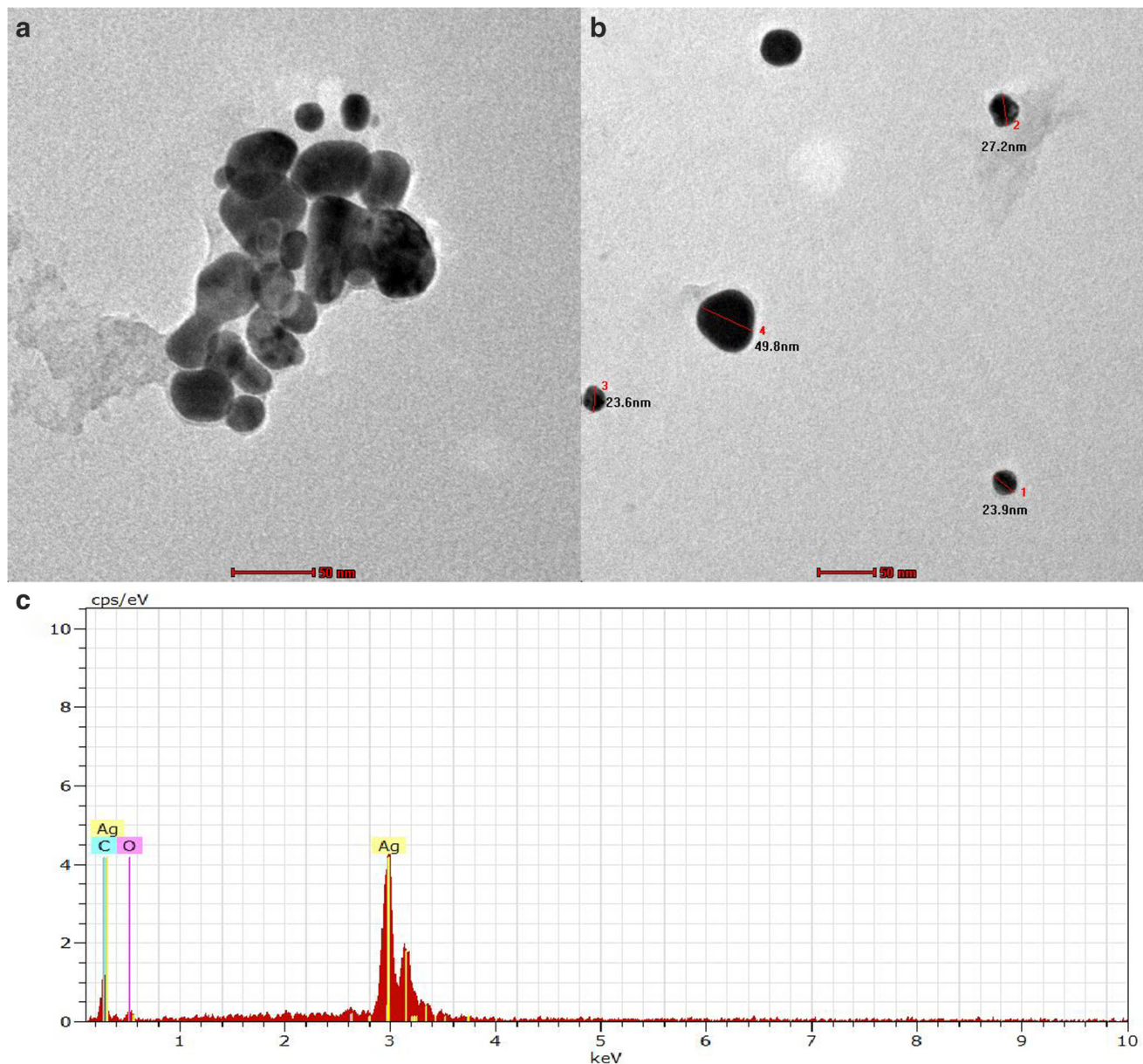


**Fig. 4** Microscopic images of biogenic AgNPs. **a** and **b** TEM analysis. **c** EDX analysis

1637  $\text{cm}^{-1}$  were assigned to the deformative vibration of water molecules. The other weak band peaks, at 2922, 1259, 1546, and 1044  $\text{cm}^{-1}$ , correspond to the stretching vibration of methyl [53], germinal methyl [54], amide I group proteins [55], and C=O stretching [56]. The characteristics peaks at 801 and 545  $\text{cm}^{-1}$  were attributed to Ag-O stretching vibration [57]. These results suggest that maybe these groups were acting as a reducing agent for the formation of AgNPs. Thus, the FT-IR study examined the presence of flavonoids, phenolics, methyl, amide groups, and proteins. Therefore, we may conclude that the biogenic AgNPs contain the phytochemical constituents.

### 3.4 TEM with EDS Analysis

TEM analysis is used to characterize the size, shape, and morphology of the synthesized nanoparticles. The size of the as-prepared NPs was 8–50 nm. Figure 4 a and b showed the spherical morphology and agglomerated silver nanoparticles [58]. Ganesh et al. [59] reported that the structure of the nanoparticles depends on the concentration of conjugating materials, which gives the shapes to the nanoparticles (spherical nature). The results were comparatively similar in the synthesis of AgNPs by using *Plukenetia volubilis* L. leaf extracts [60] and *Salvadora persica* leaf extract [61]. The energy-dispersive X-ray spectroscopy analysis (EDS) reveals a strong signal at 3 keV (Fig. 4c), which was generally exhibited by metallic silver nanocrystals due to SPR, 0.3 and 0.5 keV which originates from the un-reacted precursors of  $\text{AgNO}_3$  and biomolecules [62]. Silver (69.99%) was the major constituent element compared with carbon (22.94%) and oxygen (14.07%). The minor constituent peaks were quite normal during the green synthesis of nanoparticles [48, 63].

### 3.5 In Vitro Antioxidant Activity

Figure 5 revealed that the synthesized AgNPs exhibit radical scavenging activity (DPPH and ABTS). The radical scavenging activity tends to increase when the concentration of AgNPs showed maximum free radical scavenging activity of 73.45% (DPPH) and 57.16% (ABTS) at 100  $\mu\text{g}/\text{mL}$ . Whereas these activities were lower when compared with standard ascorbic acid, the reason behind the increased antioxidant activity was due to bioactive compounds from plant extracts [64, 65]. The study exhibits that, when the concentration of AgNPs increases, the rate of scavenging activity also increases [50]. Therefore, the antioxidant activity of AgNPs synthesized from an onion peel extract was based on the concentration-dependent manner. Using natural antioxidants can reduce the risk factors of cancer, heart disease, and chronic disorders. The present results suggest that AgNPs were a good scavenger for ROS production and have great potential for biomedical applications. Hence, biogenic AgNPs could act as an alternative antioxidant agent.

### 3.6 Antipathogenic Activity

In the study, the antipathogenic effect of synthesized AgNPs and standard antibiotic (Kanamycin) as the positive control were studied in different types of bacterial pathogens like *S. aureus*, *Bacillus* sp., *Corynebacterium* sp., *E. coli*, *Salmonella* sp., and *V. cholerae* (Fig. 6, Table 1). The AgNPs have excellent antibacterial activity against both Gram-positive (*Bacillus* sp., *S. aureus*, and *Corynebacterium* sp.) and Gram-negative (*E. coli*, *Salmonella* sp., and *V. cholerae*) bacteria. The inhibition zone increased when the concentration of AgNPs increased. The prepared AgNPs

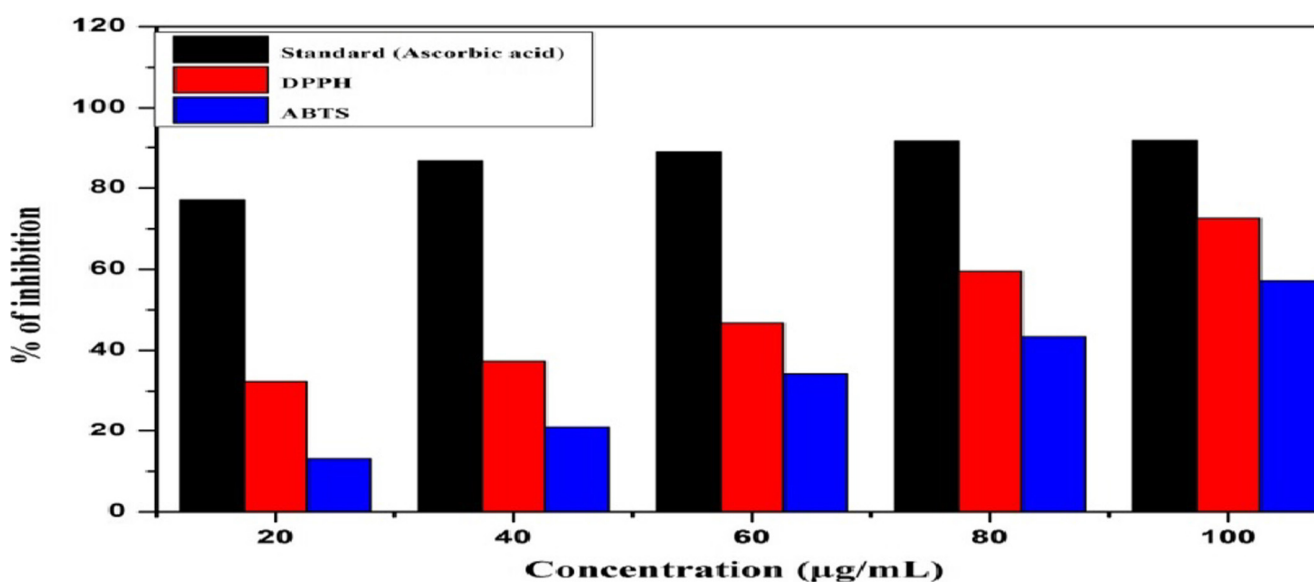
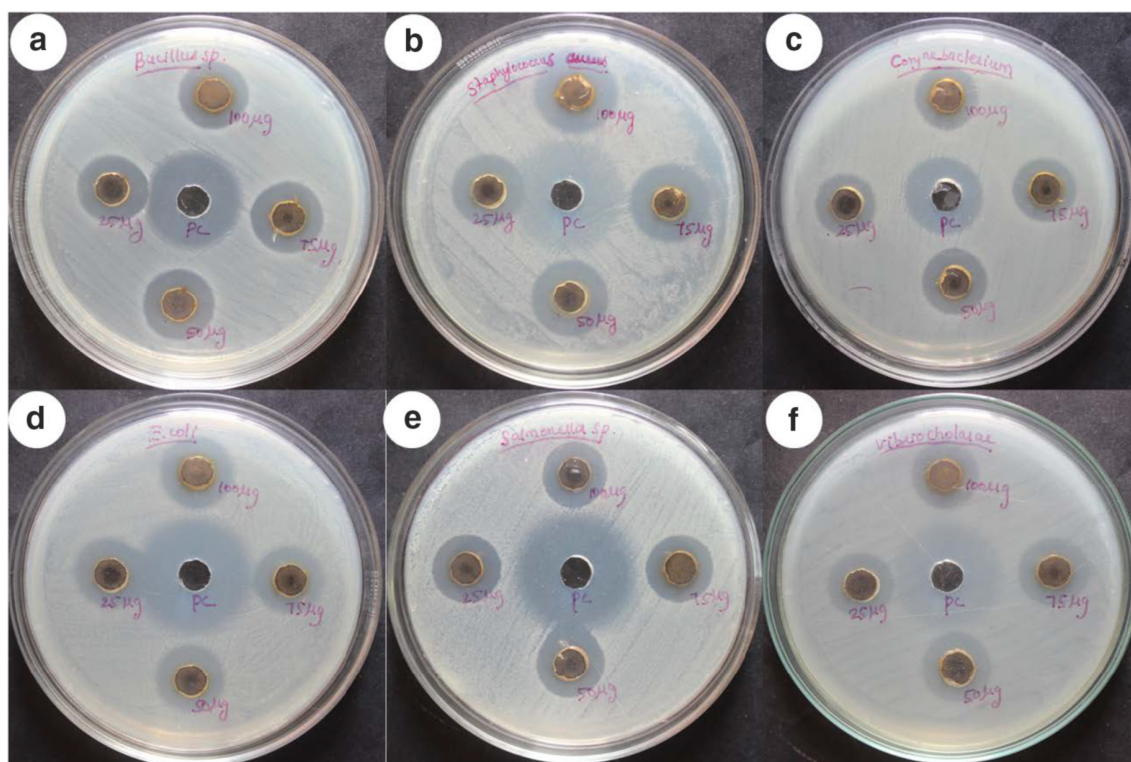


Fig. 5 In vitro antioxidant activity of AgNPs (DPPH and ABTS) with standard at different concentrations ( $\mu\text{g}/\text{ml}$ )





**Fig. 6** Antipathogenic activity of silver nanoparticles synthesized by brown skin of an onion peel extract using Gram-positive **a** *Bacillus* sp., **b** *Staphylococcus aureus* and **c** *Corynebacterium* sp. and Gram-negative **d** *E. coli*, **e** *Salmonella* sp., and **f** *Vibrio cholerae* pathogens

were more effective with the Gram-positive bacterium (*S. aureus*) than other bacterial cultures. Similar results previously reported that metallic nanoparticles inhibited the bacterial cell cycle function and bind on the active sites of the cell membrane [66, 67]. The mechanism of the antibacterial activity of AgNPs was due to the production of ROS and the release of heavy metal ions [68]. The generation of ROS such as  $\text{OH}^-$ ,  $\text{O}_2^-$ , and  $\text{H}_2\text{O}_2$  damages the outer cell membrane and inhibits bacterial growth. The released heavy metal ions ( $\text{Ag}^{2+}$ ) react with  $-\text{SH}$  group of cystine and replaces hydrogen ( $-\text{SH}$  to  $\text{S-Ag}$ ). As a result, microbes become damaged and lose their ability to multiply, which eventually leads to death [69]. Rai et al. [70] stated the AgNPs could also reduce the

bacterial metabolism and inhibit the DNA. Besides, silver ions bind with the thiol group compounds present in the respiratory enzymes of the bacterial cell wall and membrane and could be the reason for the bactericidal activity.

### 3.7 Cytotoxicity Assay

The cytotoxicity activity of AgNPs treated with A549 lung cancer cell line was investigated using MTT (3-(4,5-dimethylthiazol-2-yl)-2,5-diphenyltetrazolium bromide) cell viability assay. MTT as a tetrazolium dye reduced the mitochondrial enzymes to form a blue-colored formazan. Non-functional mitochondrial cells cannot carry out this process. Therefore,

**Table 1** Zone of inhibition of antipathogenic activity against foodborne illness-causing pathogens treated with different concentration of biogenic AgNPs

| Tested pathogens             | Zone of inhibition (mm) |  |                |                |                |
|------------------------------|-------------------------|--|----------------|----------------|----------------|
|                              | Standard                | AgNPs concentration ( $\mu\text{g/mL}$ ) |                |                |                |
|                              |                         | 25                                       | 50             | 75             | 100            |
| <i>Bacillus</i> sp.          | 21 $\pm$ 1              | 14 $\pm$ 3.5                             | 14 $\pm$ 2.8   | 16 $\pm$ 2     | 17 $\pm$ 2.5   |
| <i>Staphylococcus aureus</i> | 22 $\pm$ 2.5            | 13 $\pm$ 1.1                             | 15 $\pm$ 1.15  | 16 $\pm$ 1     | 19 $\pm$ 1     |
| <i>Corynebacterium</i> sp.   | 21 $\pm$ 1              | 14. $\pm$ 0.5                            | 14 $\pm$ 0.5   | 15 $\pm$ 0.7   | 17 $\pm$ 0.4   |
| <i>E. coli</i>               | 24.5 $\pm$ 3.6          | 14.5 $\pm$ 1.5                           | 16.3 $\pm$ 1.1 | 17.6 $\pm$ 0.5 | 19.3 $\pm$ 0.5 |
| <i>Salmonella</i> sp.        | 24.3 $\pm$ 3.4          | 13 $\pm$ 0.5                             | 14. $\pm$ 0.5  | 16 $\pm$ 1.5   | 17.7 $\pm$ 2   |
| <i>Vibrio cholerae</i>       | 24 $\pm$ 4.7            | 14.6 $\pm$ 0.5                           | 14.3 $\pm$ 0.5 | 16 $\pm$ 1.1   | 18 $\pm$ 0.5   |



the color intensity of soluble formazan was directly proportional to cell viability. In the study, AgNPs  $IC_{50}$  value ( $113.25 \pm 0.05 \mu\text{g/mL}$ ) was observed for 24 h (Fig. 7). However, in this study, AgNPs cytotoxicity activity treated with A549 lung cancer cell line remains stable after the concentration of  $40 \mu\text{g/mL}$ . For that reason, the stable cytotoxicity was due to the aggregation of AgNPs [71]. Similarly, previous studies suggest that the aggregation of nanosilver decreases the surface area and reduces reactivity [56, 72]. In addition, the cytotoxicity of the AgNPs may possibly generate the ROS, such as  $H_2O_2$ , and it was converted into a highly reactive hydroxyl or superoxide radical. Under this condition, highly reactive radicals can damage cellular components, which may lead to cell death [73, 74]. The results from the MTT assay indicated that the silver nanoparticles were cytotoxic against A549 cancer cells.

### 3.8 AO/EB Staining

The apoptotic morphological changes of A549 cell line treated with  $IC_{50}$  concentration ( $113.25 \pm 0.05 \mu\text{g/mL}$ ) of AgNPs were stained using acridine orange/ethidium bromide (dual staining). The morphological differential changes of A549 cancer cell lines were treated with biogenic AgNPs (Fig. 8a). The live cells of the control group appeared in green color (bright green fluorescence), whereas the  $IC_{50}$ -treated group appeared in orange color. The present study showed that early apoptotic features such as apoptotic bodies, cell shrinkage, chromatin condensation, necrosis, and fragmentation were observed in the AgNPs-treated cells [75]. Triggering of ROS

production in the selected cells undergoes cellular defense mechanisms and generates oxidative stress, which was defined as an imbalance between the generation of ROS and decreased antioxidant levels [76].

### 3.9 Hoechst 33258 Staining

The nuclear morphology of treated and untreated A549 cells was observed using Hoechst 33258 staining, which stains the nuclei of both the live and dead cells. Figure 8 b clearly showed that the nuclei of untreated cells were intact and rounded, but AgNPs-treated cells showed decreased normal nuclei, indicating that apoptosis was induced and the abnormal nuclei were increased. Furthermore, the AgNPs-treated cells showed cell shrinkage, chromatin condensation, and nuclear fragmentation, which was relative to the apoptosis [77, 78]. Several authors reported similar results pointed out that biogenic-synthesized nanoparticles control the cancer cell's potential [79–82]. Also, different factors such as size, surface hydrophobicity, shape, and surface area, the composition of nanoparticles, influence the cytotoxicity of nanoparticles [83].

### 3.10 Mitochondrial Membrane Potential

Mitochondrial membrane potential ( $\Delta\psi_m$ ) was a method to measure mitochondrial swelling by using mitochondrion-specific dye Rhodamine 123. Figure 8 c showed the effect of AgNPs on  $\Delta\psi_m$ . The results revealed that the control cells showed intense green fluorescence due to high mitochondrial membrane potential. In contrast, the biogenic AgNPs-treated A549 cell line showed a continuous loss of green fluorescence

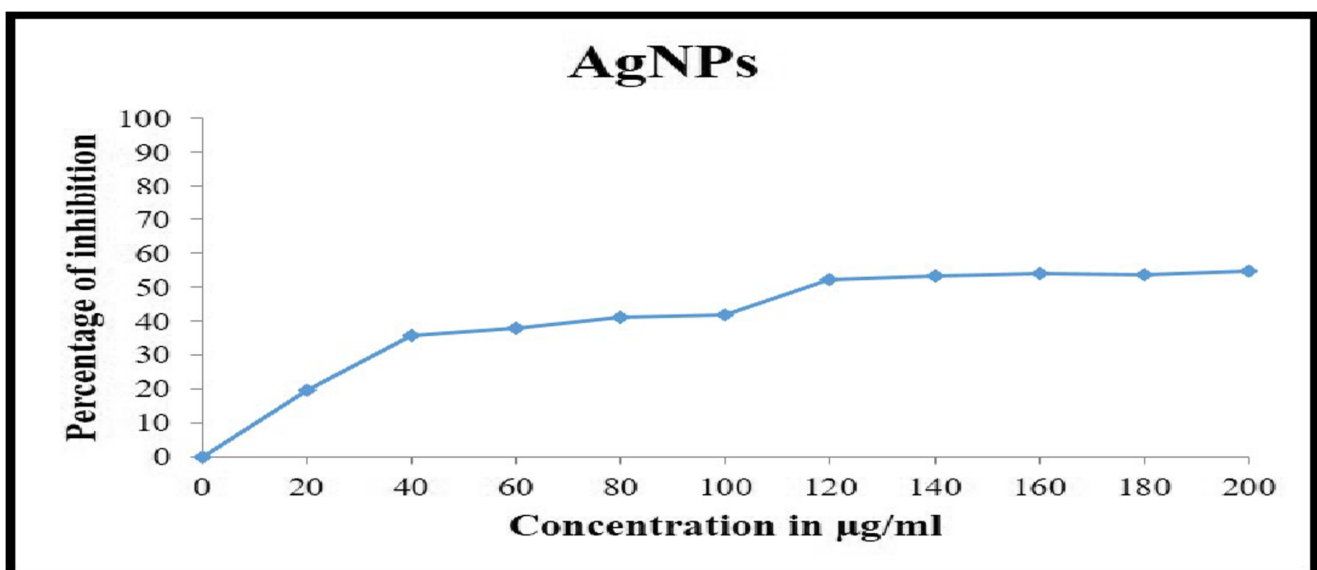
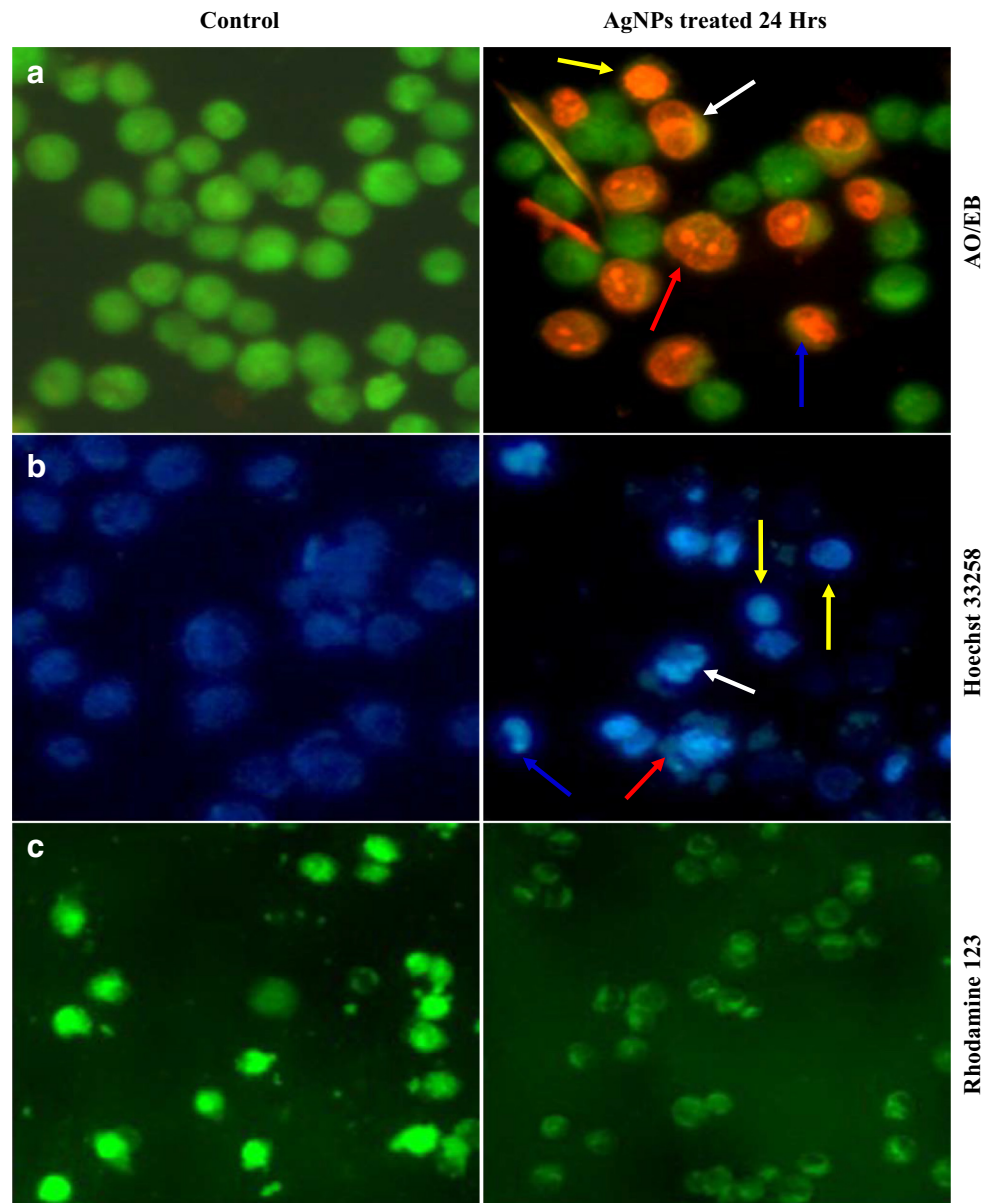


**Fig. 7** In vitro cytotoxicity assay (MTT) for AgNPs against A549 human lung cancer cell line. Cells were cultured for 24 h with different concentrations of AgNPs (0–200  $\mu\text{g/mL}$ )

**Fig. 8** Morphological changes observed for AgNPs-treated cancer cells by adopting AO/EB (a) and Hoechst 33258 (b) staining. The results showed the apoptotic bodies (red arrow), cell shrinkage (blue arrow), chromatin condensation (white arrow), and necrosis (yellow arrow), and c depict the mitochondrial membrane potential observed by Rhodamine 123 staining



due to the mitochondrial membrane depolarization, and some cells show the complete loss of mitochondrial transmembrane potential. Mollick et al. [84] reported that the function of the mitochondrial membrane potential was based on the ATP synthesis, in which the high level leads to apoptosis or necrosis. The increased level of ROS and loss of membrane integrity may be the reason for cell death by exposure of AgNPs [85].

#### 4 Conclusion

This study reports a low-cost and eco-friendly synthesis of AgNPs by applying the peel extracts of *A. cepa*. The synthesized AgNPs were in the size of 33–50 nm and spherical in morphology. This study confirmed that the

AgNPs were more effective in eradicating the generation of reactive oxygen species and free radicals, and significantly controls bacterial growth. In vitro anticancer activity results indicated that the synthesized AgNPs induces apoptosis in A549 human lung cancer cell line. The results indicate that the AgNPs synthesized by *A. cepa* (peel) can be safely applied for antibacterial and anticancer applications.

**Acknowledgments** The authors thank UGC-CPEPA National Centre for Alternatives to Animal Experiments (NCAAE) for cell culture studies in this work. The authors are grateful to UGC-SAP DRS-II and DST FIST-II for providing instrumentation facilities in the Department of Animal Science, Bharathidasan University, Tiruchirappalli – 620 024.

**Funding Information** The author K.S. Rajkumar gratefully acknowledges the Department of Science & Technology (DST), Govt. of India, for providing fellowship under the DST-INSPIRE Fellowship (IF140546).

## Compliance with Ethical Standards

**Conflict of Interest** The authors declare that they have no conflict of interest.

**Research Involving Humans and Animals Statement** None.

**Informed Consent** None.

## References

- Kim, D., Shin, K., Kwon, S. G., & Hyeon, T. (2018). Synthesis and biomedical applications of multifunctional nanoparticles. *Advanced Materials*, 30(49), 1802309. <https://doi.org/10.1002/adma.201802309>.
- Chen, G., Roy, I., Yang, C., & Prasad, P. N. (2016). Nanochemistry and nanomedicine for nanoparticle-based diagnostics and therapy. *Chemical Reviews*. <https://doi.org/10.1021/acs.chemrev.5b00148>.
- Thakkar, K. N., Mhatre, S. S., & Parikh, R. Y. (2010). *Biological synthesis of metallic nanoparticles*. Nanomedicine: Nanotechnology, Biology, and Medicine. <https://doi.org/10.1016/j.nano.2009.07.002>.
- Souayah, B., Kumar, K. G., Reddy, M. G., Rani, S., Hdhiri, N., Alfannakh, H., & Rahimi-Gorji, M. (2019). Slip flow and radiative heat transfer behavior of titanium alloy and ferromagnetic nanoparticles along with suspension of dusty fluid. *Journal of Molecular Liquids*. <https://doi.org/10.1016/j.molliq.2019.111223>.
- Kumar, K. G. (2018). Nonlinear radiative heat transfer of Cu-water nanoparticles over an unsteady rotating flow under the influence of particle shape. In B. J. Gireesha (Ed.), (p. Ch. 10). Rijeka: IntechOpen. doi:<https://doi.org/10.5772/intechopen.74807>.
- Kumar, K. G., & Archana, M. (2019). Comparative study of SiO<sub>2</sub> and TiO<sub>2</sub> nanoparticles on flow and heat transfer of dusty fluid over a stretching sheet. *Multidiscipline Modeling in Materials and Structures*. <https://doi.org/10.1108/MMMS-05-2018-0091>.
- Song, J. Y., & Kim, B. S. (2009). Rapid biological synthesis of silver nanoparticles using plant leaf extracts. *Bioprocess and Biosystems Engineering*. <https://doi.org/10.1007/s00449-008-0224-6>.
- Gleiter, H. (1990). J. Lucas, X.H. Zhang, Mater. Res. Bull. 21 (1986) 371. *Progress in Materials Science*, 33(4), 223–315. doi:[https://doi.org/10.1016/0079-6425\(89\)90001-7](https://doi.org/10.1016/0079-6425(89)90001-7).
- Patel, P., Agarwal, P., Kanawaria, S., Kachhwaha, S., & Kothari, S. L. (2015). Plant-based synthesis of silver nanoparticles and their characterization BT - nanotechnology and plant sciences: nanoparticles and their impact on plants. In M. H. Siddiqui, M. H. Al-Whaibi, & F. Mohammad (Eds.), (pp. 271–288). Cham: Springer International Publishing. [https://doi.org/10.1007/978-3-319-14502-0\\_13](https://doi.org/10.1007/978-3-319-14502-0_13).
- Reddy, M. G. G., Kumar, K. G., Shehzad, S. A., Javed, T., & Ambreen, T. (2019). Thermal transportation analysis of nanoliquid squeezed flow past a sensor surface with MCWCNT and SWCNT. *Heat Transfer-Asian Research*. <https://doi.org/10.1002/hjt.21483>.
- Rajkumar, K. S., Kanipandian, N., & Thirumurugan, R. (2016). Toxicity assessment on haematology, biochemical and histopathological alterations of silver nanoparticles-exposed freshwater fish Labeo rohita. *Applied Nanoscience (Switzerland)*. <https://doi.org/10.1007/s13204-015-0417-7>.
- Janakiraman, V., Govindarajan, K., & C R, M. (2019). Biosynthesis of silver nanoparticles from endophytic fungi, and its cytotoxic activity. *BioNanoScience*, 9(3), 573–579. doi:<https://doi.org/10.1007/s12668-019-00631-1>.
- Zheng, Y., Huang, Y., Shi, H., & Fu, L. (2019). Green biosynthesis of ZnO nanoparticles by plectranthus amboinicus leaf extract and their application for electrochemical determination of norfloxacin. *Inorganic and Nano-Metal Chemistry*, 49(9), 277–282. <https://doi.org/10.1080/24701556.2019.1661441>.
- Firdhouse, M. J., Lalitha, P., Firdhouse, M. J., & Lalitha, P. (2015). Biosynthesis of silver nanoparticles and its applications. *Journal of Nanotechnology*. <https://doi.org/10.1021/acs.macromol.7b01276>.
- Mollick, M. M. R., Bhowmick, B., Maity, D., Mondal, D., Bain, M. K., Bankura, K., et al. (2012). *Green synthesis of silver nanoparticles using Paederia foetida L. leaf extract and assessment of their antimicrobial activities*. International Journal of Green Nanotechnology: Biomedicine. <https://doi.org/10.1080/19430892.2012.706103>.
- Dobrucka, R., Dlugaszewska, J., & Kaczmarek, M. (2016). Antimicrobial and cytostatic activity of biosynthesized nanogold prepared using fruit extract of Ribes nigrum. *Arabian Journal of Chemistry*. <https://doi.org/10.1016/j.arabjc.2016.02.009>.
- Khan, A. U., Khan, M., & Khan, M. M. (2019). Antifungal and antibacterial assay by silver nanoparticles synthesized from aqueous leaf extract of Trigonella foenum-graecum. *BioNanoScience*. <https://doi.org/10.1007/s12668-019-00643-x>.
- Hamidi, A., Taghavizadeh Yazdi, M. E., Amiri, M. S., Hosseini, H. A., & Darroudi, M. (2019). Biological synthesis of silver nanoparticles in Tribulus terrestris L. extract and evaluation of their photocatalyst, antibacterial, and cytotoxicity effects. *Research on Chemical Intermediates*. doi:<https://doi.org/10.1007/s11164-019-03770-y>.
- Gajendran, B., Durai, P., Varier, K. M., Liu, W., Li, Y., Rajendran, S., et al. (2019). Green synthesis of silver nanoparticle from Datura innoxia flower extract and its cytotoxic activity. *BioNanoScience*. <https://doi.org/10.1007/s12668-019-00645-9>.
- Siddiqi, K. S., Rashid, M., Tajuddin, Husen, A., & Rehman, S. (2019). Biofabrication of silver nanoparticles from Diospyros montana, their characterization and activity against some clinical isolates. *BioNanoScience*. doi:<https://doi.org/10.1007/s12668-019-00629-9>.
- Herrera, E., Jiménez, R., Aruoma, O. I., Hercberg, S., Sánchez-García, I., & Fraga, C. (2009). Aspects of antioxidant foods and supplements in health and disease. In *Nutrition Reviews*. <https://doi.org/10.1111/j.1753-4887.2009.00177.x>.
- Moure, A., Cruz, J. M., Franco, D., Manuel Domínguez, J., Sineiro, J., Domínguez, H., et al. (2001). Natural antioxidants from residual sources. *Food Chemistry*. [https://doi.org/10.1016/S0308-8146\(00\)00223-5](https://doi.org/10.1016/S0308-8146(00)00223-5).
- Zheng, W., & Wang, S. Y. (2001). Antioxidant activity and phenolic compounds in selected herbs. *Journal of Agricultural and Food Chemistry*, 49(11), 5165–5170. <https://doi.org/10.1021/jf010697n>.
- Saha, S., Sarkar, J., Chattopadhyay, D., Patra, S., Chakraborty, A., & Acharya, K. (2010). Production of silver nanoparticles by a phytopathogenic fungus Bipolaris nodulosa and its antimicrobial activity. *Digest Journal of Nanomaterials and Biostructures*.
- Singh, A. K., Talat, M., Singh, D. P., & Srivastava, O. N. (2010). Biosynthesis of gold and silver nanoparticles by natural precursor clove and their functionalization with amine group. *Journal of Nanoparticle Research*. <https://doi.org/10.1007/s11051-009-9835-3>.
- Augusti, K. T., & Mathew, P. T. (1974). Lipid lowering effect of allicin (diallyl disulphide-oxide) on long term feeding to normal rats. *Experientia*, 30(5), 468–470. <https://doi.org/10.1007/BF01926297>.



27. Block, E. (1985). The chemistry of garlic and onions. *Scientific American*, 252(3), 114–119.
28. Griffiths, G., Trueman, L., Crowther, T., Thomas, B., & Smith, B. (2002). Onions - a global benefit to health. *Phytotherapy Research*. <https://doi.org/10.1002/ptr.1222>.
29. Dorsch, W., Wagner, H., Bayer, T., Fessler, B., Hein, G., Ring, J., ... Weiß, E. (1988). Anti-asthmatic effects of onions. Alk(enyl)sulfinothioic acid alk(enyl)-esters inhibit histamine release, leukotriene and thromboxane biosynthesis in vitro and counteract paf and allergen-induced bronchial obstruction in vivo. *Biochemical Pharmacology*. doi:[https://doi.org/10.1016/0006-2952\(88\)90663-6](https://doi.org/10.1016/0006-2952(88)90663-6).
30. Rahman, M. S. (2007). Allicin and other functional active components in garlic: health benefits and bioavailability. *International Journal of Food Properties*. <https://doi.org/10.1080/10942910601113327>.
31. Benitez, V., Molla, E., Martin-Cabrejas, M. A., Aguilera, Y., Lopez-Andreu, F. J., Cools, K., et al. (2011). Characterization of industrial onion wastes (*Allium cepa* L.): dietary fibre and bioactive compounds. *Plant foods for human nutrition (Dordrecht, Netherlands)*, 66(1), 48–57. <https://doi.org/10.1007/s11130-011-0212-x>.
32. Prakash, D., Singh, B. N., & Upadhyay, G. (2007). Antioxidant and free radical scavenging activities of phenols from onion (*Allium cepa*). *Food Chemistry*. <https://doi.org/10.1016/j.foodchem.2006.06.063>.
33. Nuutila, A. M., Puupponen-Pimiä, R., Aarni, M., & Oksman-Caldentey, K. M. (2003). Comparison of antioxidant activities of onion and garlic extracts by inhibition of lipid peroxidation and radical scavenging activity. *Food Chemistry*. [https://doi.org/10.1016/S0308-8146\(02\)00476-4](https://doi.org/10.1016/S0308-8146(02)00476-4).
34. Sahni, G., Panwar, A., & Kaur, B. (2015). Controlled green synthesis of silver nanoparticles by *Allium cepa* and *Musa acuminata* with strong antimicrobial activity. *International Nano Letters*. <https://doi.org/10.1007/s40089-015-0142-y>.
35. Khalilzadeh, M. A., & Borzoo, M. (2016). Green synthesis of silver nanoparticles using onion extract and their application for the preparation of a modified electrode for determination of ascorbic acid. *Journal of Food and Drug Analysis*. <https://doi.org/10.1016/j.jfda.2016.05.004>.
36. Kim, J., Cha, Y. J., Lee, K. H., & Park, E. (2013). Effect of onion peel extract supplementation on the lipid profile and antioxidative status of healthy young women: a randomized, placebo-controlled, double-blind, crossover trial. *Nutrition Research and Practice*. <https://doi.org/10.4162/nrp.2013.7.5.373>.
37. Brand-Williams, W., Cuvelier, M. E., & Berset, C. (1995). Use of a free radical method to evaluate antioxidant activity. *LWT - Food Science and Technology*. [https://doi.org/10.1016/S0023-6438\(95\)80008-5](https://doi.org/10.1016/S0023-6438(95)80008-5).
38. Re, R., Pellegrini, N., Proteggente, A., Pannala, A., Yang, M., & Rice-Evans, C. (1999). Antioxidant activity applying an improved ABTS radical cation decolorization assay. *Free Radical Biology and Medicine*. [https://doi.org/10.1016/S0891-5849\(98\)00315-3](https://doi.org/10.1016/S0891-5849(98)00315-3).
39. Mosmann, T. (1983). Rapid colorimetric assay for cellular growth and survival: application to proliferation and cytotoxicity assays. *Journal of Immunological Methods*. [https://doi.org/10.1016/0022-1759\(83\)90303-4](https://doi.org/10.1016/0022-1759(83)90303-4).
40. Spector, D. L., Goldman, R. D., & Leinwand, L. A. (1998). Cells: a laboratory manual. Volume 1, Volume 1., Plainview, N.Y.: Cold Spring Harbor Laboratory Press.
41. Kasibhatla, S. (2006). Staining of suspension cells with Hoechst 33258 to detect apoptosis. *Cold Spring Harbor Protocols*. <https://doi.org/10.1101/pdb.prot4492>.
42. Baracca, A., Sgarbi, G., Solaini, G., & Lenaz, G. (2003). Rhodamine 123 as a probe of mitochondrial membrane potential: evaluation of proton flux through F0 during ATP synthesis. *Biochimica et Biophysica Acta - Bioenergetics*. [https://doi.org/10.1016/S0005-2728\(03\)00110-5](https://doi.org/10.1016/S0005-2728(03)00110-5).
43. Joerger, R., Klaus, T., & Granqvist, C. G. (2000). Biologically produced silver-carbon composite materials for optically functional thin-film coatings. *Advanced Materials*. [https://doi.org/10.1002/\(SICI\)1521-4095\(200003\)12:6<407::AID-ADMA407>3.0.CO;2-O](https://doi.org/10.1002/(SICI)1521-4095(200003)12:6<407::AID-ADMA407>3.0.CO;2-O).
44. Klaus, T., Joerger, R., Olsson, E., & Granqvist, C.-G. (2002). Silver-based crystalline nanoparticles, microbially fabricated. *Proceedings of the National Academy of Sciences*. <https://doi.org/10.1073/pnas.96.24.13611>.
45. Mukherjee, P., Ahmad, A., Mandal, D., Senapati, S., Sainkar, S. R., Khan, M. I., ... Sastry, M. (2001). Fungus-mediated synthesis of silver nanoparticles and their immobilization in the mycelial matrix: a novel biological approach to nanoparticle synthesis. *Nano Letters*. doi:<https://doi.org/10.1021/nl0155274>.
46. Ahmad, A., Mukherjee, P., Senapati, S., Mandal, D., Khan, M. I., Kumar, R., & Sastry, M. (2003). Extracellular biosynthesis of silver nanoparticles using the fungus *Fusarium oxysporum*. *Colloids and Surfaces B: Biointerfaces*, 28(4), 313–318. [https://doi.org/10.1016/S0927-7765\(02\)00174-1](https://doi.org/10.1016/S0927-7765(02)00174-1).
47. He, Y., Du, Z., Ma, S., Cheng, S., Jiang, S., Liu, Y., ... Zheng, X. (2016). Biosynthesis, antibacterial activity and anticancer effects against prostate cancer (PC-3) cells of silver nanoparticles using *Dimocarpus Longan* Lour. peel extract. *Nanoscale Research Letters*. doi:<https://doi.org/10.1186/s11671-016-1511-9>.
48. Ahmed, M. J., Murtaza, G., Mehmood, A., & Bhatti, T. M. (2015). Green synthesis of silver nanoparticles using leaves extract of *Skimmia laureola*: characterization and antibacterial activity. *Materials Letters*. <https://doi.org/10.1016/j.matlet.2015.03.143>.
49. Gurunathan, S., Raman, J., Abd Malek, S. N., John, P. A., & Vikineswary, S. (2013). Green synthesis of silver nanoparticles using *Ganoderma neo-japonicum* Imazeki: a potential cytotoxic agent against breast cancer cells. *International Journal of Nanomedicine*. doi:<https://doi.org/10.2147/IJN.S51881>.
50. Kanipandian, N., & Thirumurugan, R. (2014). A feasible approach to phyto-mediated synthesis of silver nanoparticles using industrial crop *Gossypium hirsutum* (cotton) extract as stabilizing agent and assessment of its in vitro biomedical potential. *Industrial Crops and Products*, 55, 1–10. <https://doi.org/10.1016/j.indcrop.2014.01.042>.
51. Sondi, I., & Salopek-Sondi, B. (2004). Silver nanoparticles as antimicrobial agent: a case study on *E. coli* as a model for Gram-negative bacteria. *Journal of Colloid and Interface Science*. doi:<https://doi.org/10.1016/j.jcis.2004.02.012>.
52. Venkatpurwar, V., & Pokharkar, V. (2011). Green synthesis of silver nanoparticles using marine polysaccharide: study of in-vitro antibacterial activity. *Materials Letters*. <https://doi.org/10.1016/j.matlet.2010.12.057>.
53. Li, S., Shen, Y., Xie, A., Yu, X., Qiu, L., Zhang, L., & Zhang, Q. (2007). Green synthesis of silver nanoparticles using *Capsicum annuum* L. extract. *Green Chemistry*. doi:<https://doi.org/10.1039/b615357g>.
54. Tripathy, A., Raichur, A. M., Chandrasekaran, N., Prathna, T. C., & Mukherjee, A. (2010). Process variables in biomimetic synthesis of silver nanoparticles by aqueous extract of *Azadirachta indica* (Neem) leaves. *Journal of Nanoparticle Research*. <https://doi.org/10.1007/s11051-009-9602-5>.
55. Whiteman, S. C., Yang, Y., Jones, J. M., & Spiteri, M. A. (2008). FTIR spectroscopic analysis of sputum: preliminary findings on a potential novel diagnostic marker for COPD. *Therapeutic Advances*



- in Respiratory Disease*, 2(1), 23–31. <https://doi.org/10.1177/1753465807087972>.
56. Jain, N., Bhargava, A., Majumdar, S., Tarafdar, J. C., & Panwar, J. (2011). Extracellular biosynthesis and characterization of silver nanoparticles using *Aspergillus flavus* NJP08: a mechanism perspective. *Nanoscale*. <https://doi.org/10.1039/c0nr00656d>.
  57. Ghaseminezhad, S. M., Hamed, S., & Shojaosadati, S. A. (2012). Green synthesis of silver nanoparticles by a novel method: comparative study of their properties. *Carbohydrate Polymers*. <https://doi.org/10.1016/j.carbpol.2012.03.030>.
  58. Abdel-Aziz, M. S., Shaheen, M. S., El-Nekeety, A. A., & Abdel-Wahhab, M. A. (2014). Antioxidant and antibacterial activity of silver nanoparticles biosynthesized using *Chenopodium murale* leaf extract. *Journal of Saudi Chemical Society*. <https://doi.org/10.1016/j.jscs.2013.09.011>.
  59. Kumar, K. G., Avinash, B. S., Rahimi-Gorji, M., & Alarifi, I. M. (2019). Optical and electrical properties of Ti1-XSnXO2 nanoparticles. *Journal of Molecular Liquids*, 293, 111556. <https://doi.org/10.1016/j.molliq.2019.111556>.
  60. Kumar, B., Smita, K., Cumbal, L., & Debut, A. (2014). Synthesis of silver nanoparticles using *Sacha inchi* (*Plukenetia volubilis* L.) leaf extracts. *Saudi Journal of Biological Sciences*. doi:<https://doi.org/10.1016/j.sjbs.2014.07.004>.
  61. A. Alshaye, N., M. Elobeid, M., H.M. Alkha, D., & E. Mohamme, A. (2016). Characterization of biogenic silver nanoparticles by *Salvadora persica* leaves extract and its application against some MDR pathogens *E. coli* and *S. aureus*. *Research Journal of Microbiology*. doi:<https://doi.org/10.3923/jm.2017.74.81>.
  62. Kanipandian, N., Kannan, S., Ramesh, R., Subramanian, P., & Thirumurugan, R. (2014). Characterization, antioxidant and cytotoxicity evaluation of green synthesized silver nanoparticles using *Cleistanthus collinus* extract as surface modifier. *Materials Research Bulletin*. <https://doi.org/10.1016/j.materresbull.2013.09.016>.
  63. Rai, A., Singh, A., Ahmad, A., & Sastry, M. (2006). Role of halide ions and temperature on the morphology of biologically synthesized gold nanotriangles. *Langmuir*. <https://doi.org/10.1021/la052055q>.
  64. Mittal, A. K., Bhaumik, J., Kumar, S., & Banerjee, U. C. (2014). Biosynthesis of silver nanoparticles: elucidation of prospective mechanism and therapeutic potential. *Journal of Colloid and Interface Science*, 415, 39–47. <https://doi.org/10.1016/j.jcis.2013.10.018>.
  65. Kumar, B., Smita, K., Seqqat, R., Benalcazar, K., Grijalva, M., & Cumbal, L. (2016). In vitro evaluation of silver nanoparticles cytotoxicity on hepatic cancer (Hep-G2) cell line and their antioxidant activity: green approach for fabrication and application. *Journal of Photochemistry and Photobiology B: Biology*. <https://doi.org/10.1016/j.jphotobiol.2016.03.011>.
  66. Selvam, K., Sudhakar, C., Govarthanan, M., Thiyagarajan, P., Sengottaiyan, A., Senthilkumar, B., & Selvankumar, T. (2017). Eco-friendly biosynthesis and characterization of silver nanoparticles using *Tinospora cordifolia* (Thunb.) Miers and evaluate its antibacterial, antioxidant potential. *Journal of Radiation Research and Applied Sciences*. doi:<https://doi.org/10.1016/j.jrras.2016.02.005>.
  67. Kim, J. S., Kuk, E., Yu, K. N., Kim, J. H., Park, S. J., Lee, H. J., et al. (2007). *Antimicrobial effects of silver nanoparticles*. *Nanomedicine: Nanotechnology, Biology, and Medicine*. <https://doi.org/10.1016/j.nano.2006.12.001>.
  68. Karthik, K., Dhanuskodi, S., Gobinath, C., & Sivaramakrishnan, S. (2015). Microwave-assisted synthesis of CdO-ZnO nanocomposite and its antibacterial activity against human pathogens. *Spectrochimica Acta - Part A: Molecular and Biomolecular Spectroscopy*. <https://doi.org/10.1016/j.saa.2014.11.079>.
  69. Hoskote Anand, K. K., & Mandal, B. K. (2015). Activity study of biogenic spherical silver nanoparticles towards microbes and oxidants. *Spectrochimica Acta - Part A: Molecular and Biomolecular Spectroscopy*. <https://doi.org/10.1016/j.saa.2014.07.013>.
  70. Rai, M., Yadav, A., & Gade, A. (2009). Silver nanoparticles as a new generation of antimicrobials. *Biotechnology Advances*. <https://doi.org/10.1016/j.biotechadv.2008.09.002>.
  71. Justin Packia Jacob, S., Finub, J. S., & Narayanan, A. (2012). Synthesis of silver nanoparticles using *Piper longum* leaf extracts and its cytotoxic activity against Hep-2 cell line. *Colloids and Surfaces B: Biointerfaces*. <https://doi.org/10.1016/j.colsurfb.2011.11.001>.
  72. Thakore, S. I., Nagar, P. S., Jadeja, R. N., Thounaojam, M., Devkar, R. V., & Rathore, P. S. (2019). Sapota fruit latex mediated synthesis of Ag, Cu mono and bimetallic nanoparticles and their in vitro toxicity studies. *Arabian Journal of Chemistry*. doi:<https://doi.org/10.1016/j.arabjc.2014.12.042>.
  73. Manke, A., Wang, L., & Rojanasakul, Y. (2013). Mechanisms of nanoparticle-induced oxidative stress and toxicity. *BioMed Research International*. <https://doi.org/10.1155/2013/942916>.
  74. Aadil, K. R., Pandey, N., Mussatto, S. I., & Jha, H. (2019). Green synthesis of silver nanoparticles using acacia lignin, their cytotoxicity, catalytic, metal ion sensing capability and antibacterial activity. *Journal of Environmental Chemical Engineering*. <https://doi.org/10.1016/j.jece.2019.103296>.
  75. Azandeh, S. S., Abbaspour, M., Khodadadi, A., Khorsandi, L., Orazizadeh, M., & Heidari-Moghadam, A. (2017). Anticancer activity of curcumin-loaded PLGA nanoparticles on PC3 prostate cancer cells. *Iranian Journal of Pharmaceutical Research*.
  76. Roessner, A., Kuester, D., Malfertheiner, P., & Schneider-Stock, R. (2008). Oxidative stress in ulcerative colitis-associated carcinogenesis. *Pathology Research and Practice*. <https://doi.org/10.1016/j.prp.2008.04.011>.
  77. Behboodi, S., Baghbani-Arani, F., Abdalan, S., & Sadat Shandiz, S. A. (2019). Green engineered biomolecule-capped silver nanoparticles fabricated from *Cichorium intybus* extract: in vitro assessment on apoptosis properties toward human breast cancer (MCF-7) cells. *Biological Trace Element Research*. <https://doi.org/10.1007/s12011-018-1392-0>.
  78. Akther, T., Mathipi, V., Kumar, N. S., Davoodbasha, M., & Srinivasan, H. (2019). Fungal-mediated synthesis of pharmaceutically active silver nanoparticles and anticancer property against A549 cells through apoptosis. *Environmental Science and Pollution Research*. <https://doi.org/10.1007/s11356-019-04718-w>.
  79. Sivagami, G., Vinothkumar, R., Preethy, C. P., Riyasdeen, A., Akbarsha, M. A., Menon, V. P., & Nalini, N. (2012). Role of hesperetin (a natural flavonoid) and its analogue on apoptosis in HT-29 human colon adenocarcinoma cell line - a comparative study. *Food and Chemical Toxicology*. <https://doi.org/10.1016/j.fct.2011.11.038>.
  80. Kim, C. G., Castro-Aceituno, V., Abbai, R., Lee, H. A., Simu, S. Y., Han, Y., et al. (2018). Caspase-3/MAPK pathways as main regulators of the apoptotic effect of the phyto-mediated synthesized silver nanoparticle from dried stem of *Eleutherococcus senticosus* in human cancer cells. *Biomedicine & Pharmacotherapy*, 99, 128–133. <https://doi.org/10.1016/j.biopha.2018.01.050>.
  81. Plackal Adimuriyil George, B., Kumar, N., Abrahamse, H., & Ray, S. S. (2018). Apoptotic efficacy of multifaceted biosynthesized silver nanoparticles on human adenocarcinoma cells. *Scientific Reports*. <https://doi.org/10.1038/s41598-018-32480-5>.

82. Wang, C., Mathiyalagan, R., Kim, Y. J., Castro-Aceituno, V., Singh, P., Ahn, S., et al. (2016). Rapid green synthesis of silver and gold nanoparticles using *Dendropanax morbifera* leaf extract and their anticancer activities. *International Journal of Nanomedicine*. <https://doi.org/10.2147/IJN.S97181>.
83. Fröhlich, E. (2012). The role of surface charge in cellular uptake and cytotoxicity of medical nanoparticles. *International Journal of Nanomedicine*. <https://doi.org/10.2147/IJN.S36111>.
84. Rahaman Mollick, M. M., Bhowmick, B., Mondal, D., Maity, D., Rana, D., Dash, S. K., ... Chattopadhyay, D. (2014). Anticancer (in vitro) and antimicrobial effect of gold nanoparticles synthesized using *Abelmoschus esculentus* (L.) pulp extract via a green route. *RSC Advances*. doi:<https://doi.org/10.1039/c4ra07285e>.
85. Jeyaraj, M., Rajesh, M., Arun, R., MubarakAli, D., Sathishkumar, G., Sivanandhan, G., et al. (2013). An investigation on the cytotoxicity and caspase-mediated apoptotic effect of biologically synthesized silver nanoparticles using *Podophyllum hexandrum* on human cervical carcinoma cells. *Colloids and Surfaces B: Biointerfaces*. <https://doi.org/10.1016/j.colsurfb.2012.09.042>.

**Publisher's Note** Springer Nature remains neutral with regard to jurisdictional claims in published maps and institutional affiliations.